Crystallography.

Single crystal X-ray data of **1** were collected at 300, 250, 120 and 92 K on a Xcalibur, Sapphire3, Gemini diffractometer equipped with a graphite-monochromated Enhance (Mo) X-ray Source (λ = 0.71073 Å). The program CrysAlisPro, Oxford Diffraction Ltd., Version 1.171.33.52 was used for cell refinements and data reduction of the compound. Empirical absorption correction was performed using spherical harmonics, implemented in SCALE3 ABSPACK scaling algorithm. Crystal structures were solved by direct methods with the SIR97 program,[1] and refined against all F^2 values with the SHELXL-97 program,[2] using the WinGX graphical user interface.[3] Non-hydrogen atoms were refined anisotropically (except as noted), and hydrogen atoms were placed in calculated positions refined using idealized geometries (riding model) and assigned fixed isotropic displacement parameters.

Table S1. List of atoms from $[Fe(sal_2\text{-}trien)]^+$ with short contacts in the estructure at 300 K

With the oxalate network	with other $[Fe(sal_2\text{-}trien)]^+$ cations	π-π stacking interactions
d_{C14-O9}=3.196 Å	$d_{C15-C17}$=3.706 Å	d_{C5-C6}=3.555 Å
d_{C13-O6}=3.498 Å	$d_{C10B-C16}$=3.646 Å	d_{C4-C7}=3.569 Å
$d_{C11A-O11}$=3.399 Å	$d_{C10B-C17}$=3.566 Å	d_{C3-C3*}=3.405 Å
d_{C9-O4}=3.436 Å	$d_{C17-C20}$=3.545 Å	
d_{C7-O8}=3.310 Å	d_{C17-N2}=3.492 Å	
d_{C5-O12}=3.347 Å		
d_{C2-O15}=3.474 Å		

Table S2. List of atoms from $[Fe(sal_2\text{-}trien)]^+$ with short contacts in the estructure at 120 K

With the oxalate network	with other $[Fe(sal_2\text{-}trien)]^+$ cations	π-π stacking interactions
d_{C19-O9}=3.555 Å	d_{N2-C16}=3.665 Å	d_{C5-C6}=3.544 Å
d_{C16-O4}=3.537 Å	$d_{C15-C17}$=3.700 Å	d_{C4-C7}=3.454 Å
d_{C14-O7}=3.141 Å	$d_{C10-C17}$=3.585 Å	d_{C3-C3*}=3.634 Å
d_{C13-O4}=3.328 Å	$d_{C17-C20}$=3.579 Å	
$d_{C12-O15}$=3.259 Å	d_{C17-N2}=3.342 Å	
$d_{C11-O15}$=3.114 Å		
d_{C9-O6}=3.474 Å		
d_{C5-O16}=3.354 Å		
d_{C2-O11}=3.367 Å		

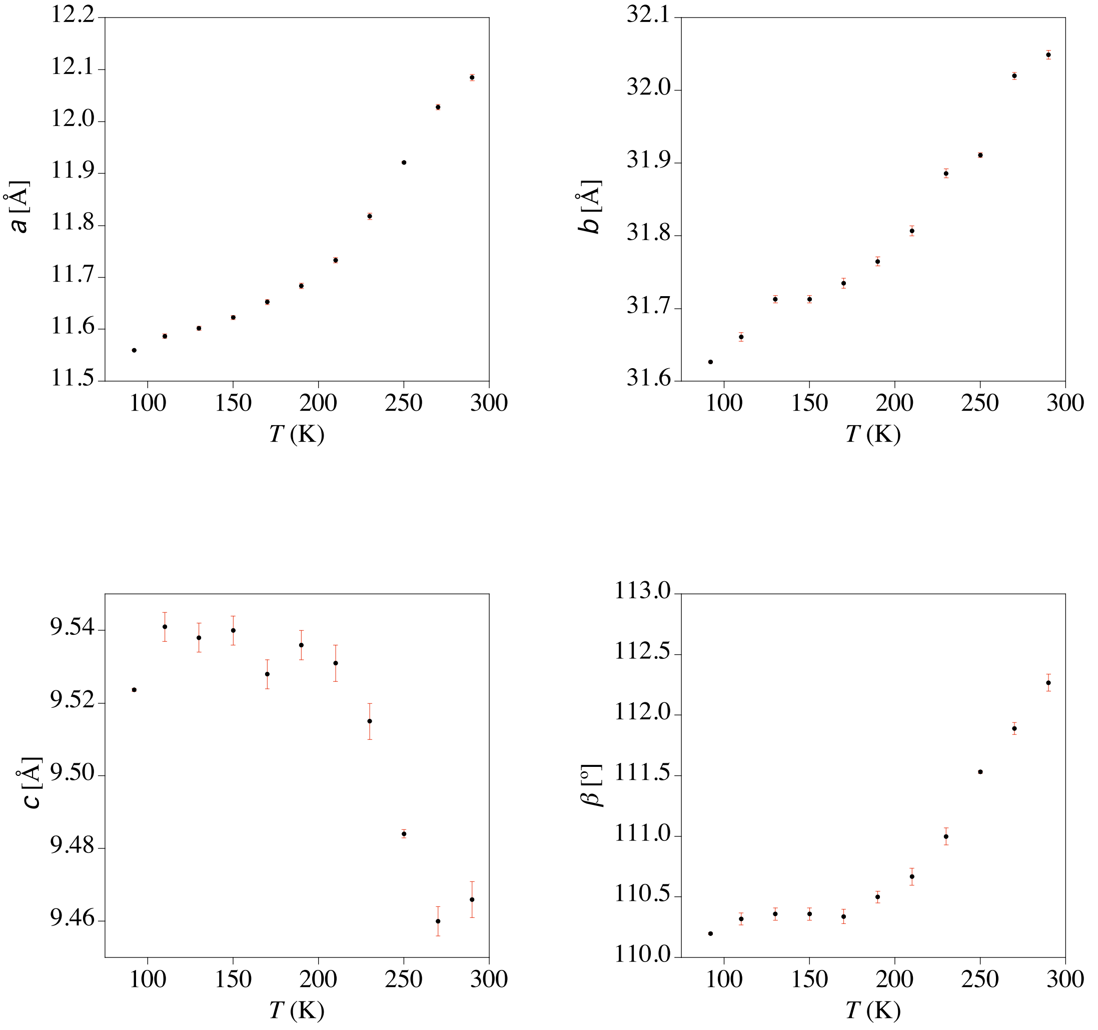

Figure S1. Plots of the cell dimensions *a* (Å), *b* (Å), *c* (Å) and *β* (°) for **1** determined from 290 to 92 K at –20 K intervals.

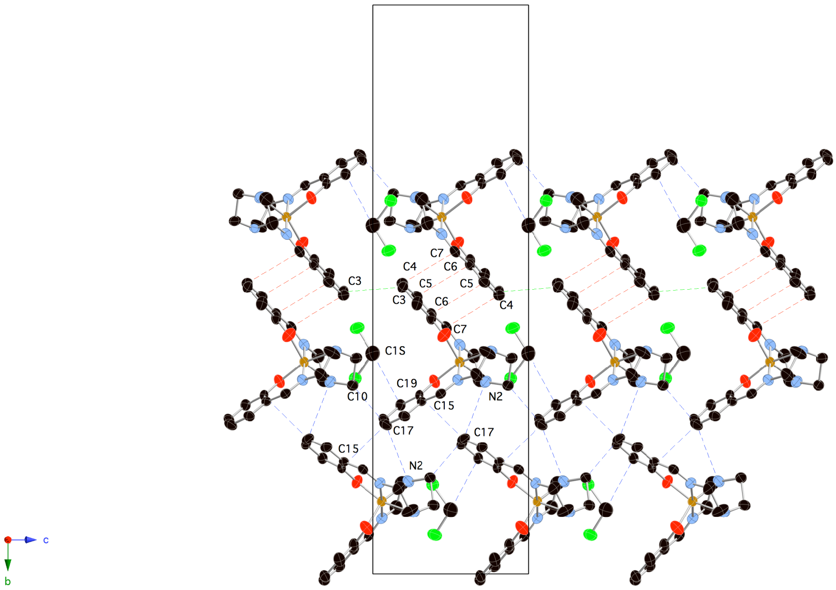

Figure S2. Molecular packing of [Fe(sal$_2$-trien)]$^+$ cations in **1** at 300 K (dashed blue lines are intrachain contacts; dashed red lines are interchain contacts; dashed green lines are π–π stacking interactions between C atoms from different chains. Fe (yellow), Cl (green) C (black), N (blue), O (red). Hydrogen atoms have been omitted for clarity).

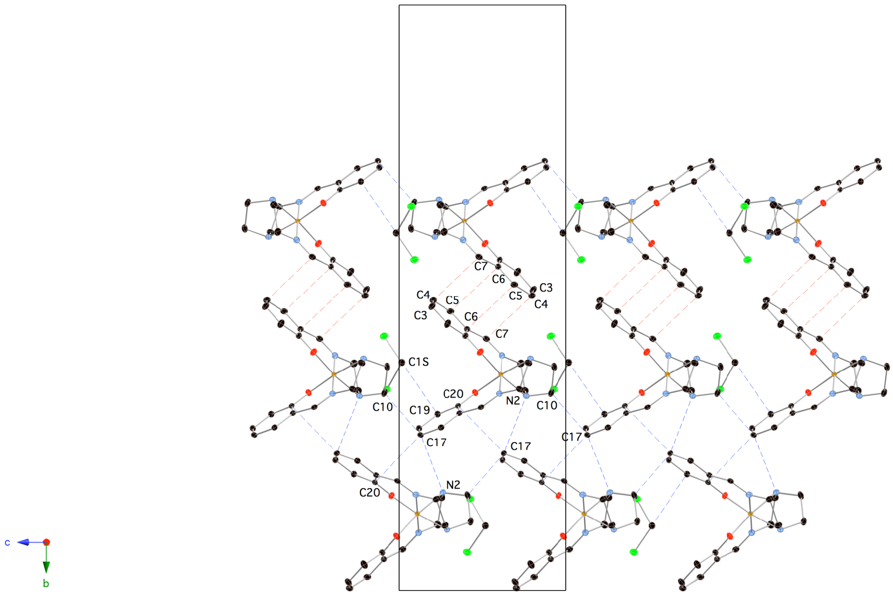

Figure S3. Molecular packing of $[Fe(sal_2\text{-trien})]^+$ cations in **1** at 120 K (dashed blue lines are intrachain contacts; dashed red lines are interchain contacts; Fe (yellow), Cl (green) C (black), N (blue), O (red)). Hydrogen atoms have been omitted for clarity).

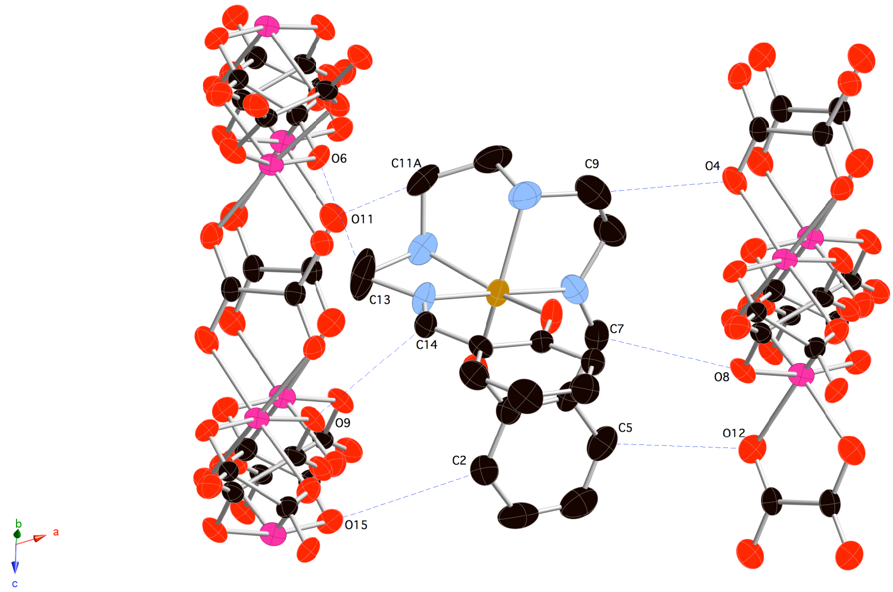

Figure S4. Short contacts between [Fe(sal$_2$-trien)]$^+$ cations and oxalate ligands in **1** at 300 K (dashed blue lines are short contacts; Fe (yellow), C (black), N (blue), O (red), Mn/Cr (pink). Hydrogen atoms have been omitted for clarity).

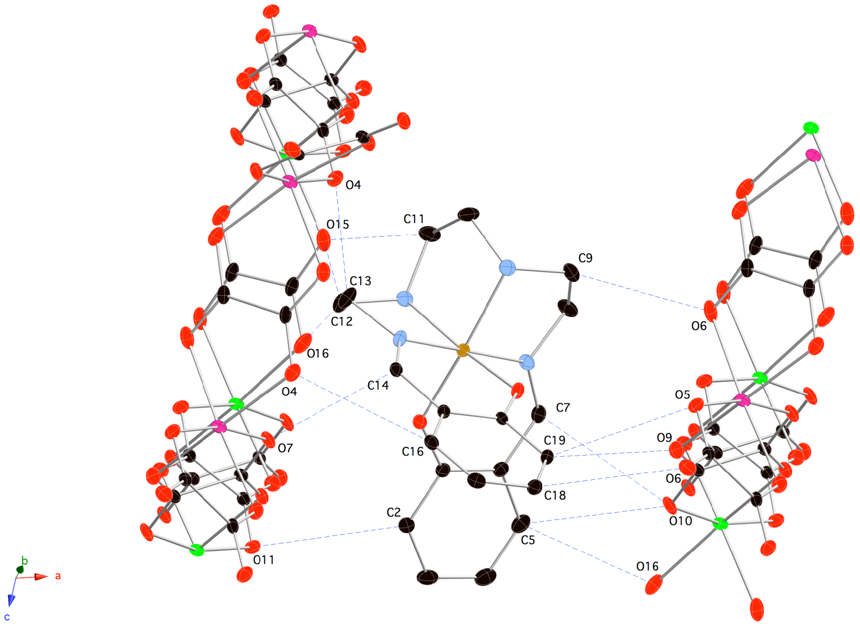

Figure S5. Short contacts between [Fe(sal$_2$-trien)]$^+$ cations and oxalate ligands in **1** at 120 K (dashed blue lines are short contacts; Fe (yellow), C (black), N (blue), O (red), Mn/Cr (pink). Hydrogen atoms have been omitted for clarity).

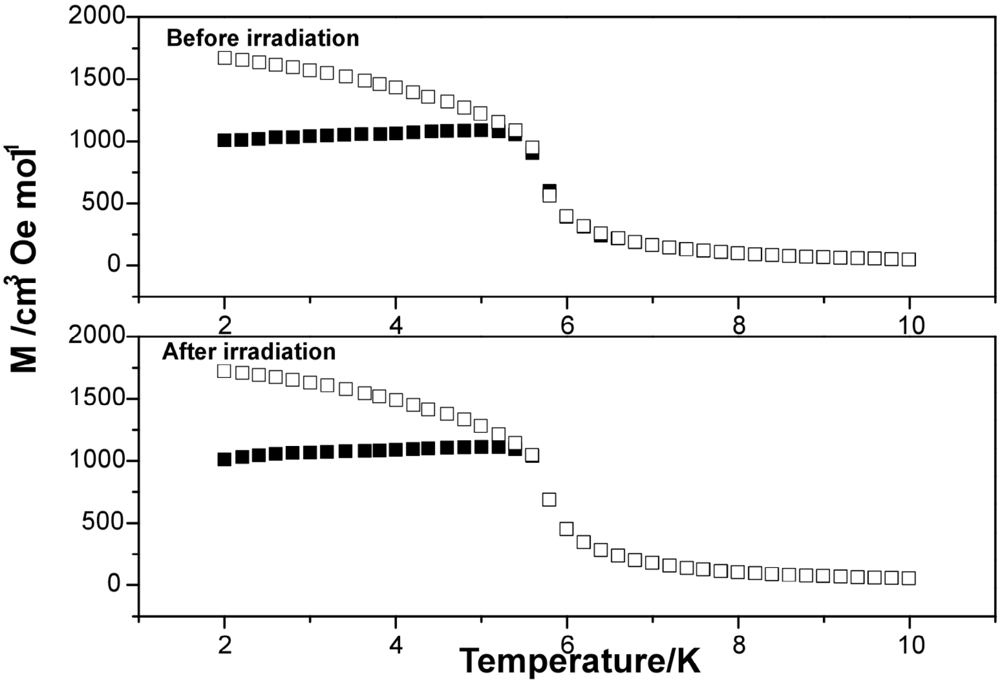

Figure S6. Field cooled (FC) and zero-field cooled (ZFC) magnetization measurements of **1** with an applied field of 20 Oe before and after irradiation. (□ FC ■ ZFC).

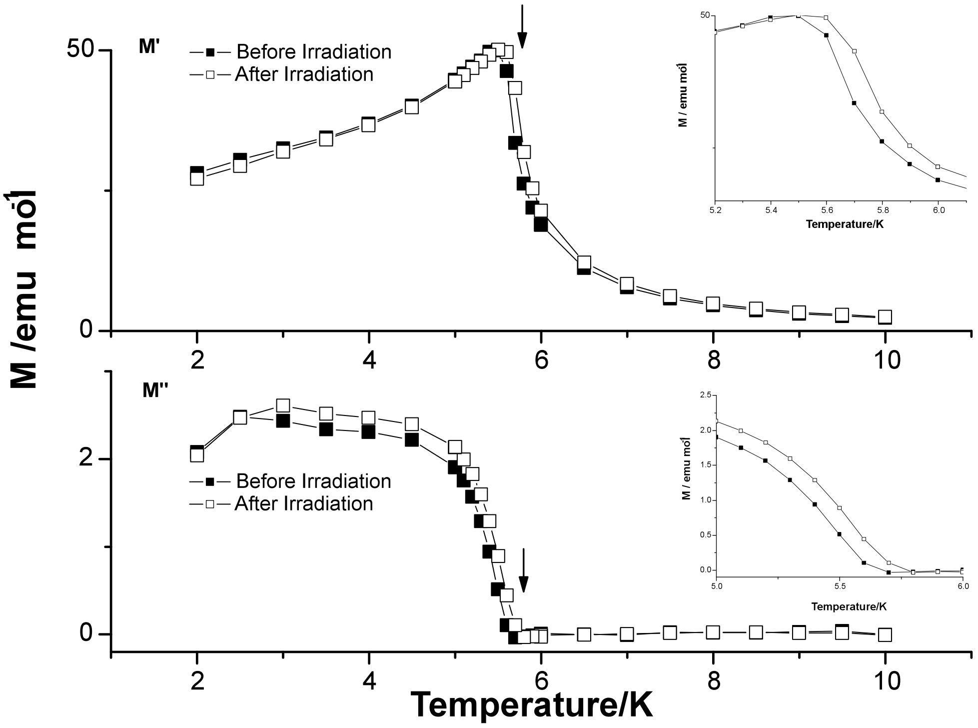

Figure S7. AC measurement (3.8 Oe oscillating field with frequency of 100 Hz) of **1** before and after irradiation (■ Before irradiation, □ After irradiation).

Details of the fitting of the magnetism of $[\mathrm{Mn^{II}Cr^{III}(ox)_3}]$ layers.

The χT product of compound **1** can be decomposed as the sum of three components : the χT component of the magnetic layers $[\mathrm{Mn^{II}Cr^{III}(ox)_3}]$, noted hereafter $\chi T(\mathrm{MnCr})$, the χT product for HS Fe(III), $\chi T(\mathrm{Fe^{III}\text{-}HS})$], multiplied by high spin fraction γ_{HS}, and the χT product for LS Fe(III), χT $(\mathrm{Fe^{III}\text{-}LS})$], multiplied by low spin fraction $1\text{-}\gamma_{\mathrm{HS}}$:

$\chi T = \chi T(\mathrm{MnCr}) + \chi T(\mathrm{Fe^{III}\text{-}HS})\ \gamma_{\mathrm{HS}} + \chi T(\mathrm{Fe^{III}\text{-}LS})(1\text{-}\gamma_{\mathrm{HS}})$. When the Fe(III) centre is in its low spin state ($\gamma_{\mathrm{HS}} = 0$), the χT ($\gamma_{\mathrm{HS}} = 0$) product is the sum of the contributions of $[\mathrm{Mn^{II}Cr^{III}(ox)_3}]$ layers and low spin Fe(III): χT $(\gamma_{\mathrm{HS}} = 0) = \chi T(\mathrm{MnCr}) + \chi T(\mathrm{Fe^{III}\text{-}LS})$.

Below the thermal spin transition (i.e. below 150 K) and well above the Curie temperature (i.e. above 50 K), the magnetic response can be satisfactorily simulated by a Curie-Weiss law, i.e. $\chi(\gamma_{HS} = 0) = \dfrac{C}{T - \theta}$.

Inserted graph in figure 3 shows the linear fit of the Curie Weiss Law. The deduced parameters are C = 6.93 $\mathrm{cm^3\ K\ mol^{-1}}$ and θ = 7.98 K. The positive θ indicates a ferromagnetic Cr-Mn interaction. Taking Curie constants as 4.375 for $\mathrm{Mn^{II}}$, 1.875 for $\mathrm{Cr^{III}}$ and 0.6 $\mathrm{cm^3\ K\ mol^{-1}}$ for LS $\mathrm{Fe^{III}}$ respectively leads to an expected C value of 6.85 $\mathrm{cm^3\ K\ mol^{-1}}$ for the compound, in excellent agreement with the experimental one. It should nevertheless be emphasized that the C value, and consequently the magnetism simulated between 50 and 150 K, takes into account not only the magnetism of $[\mathrm{Mn^{II}Cr^{III}(ox)_3}]$ layers but also the magnetism of LS $\mathrm{Fe^{III}}$ (S=1/2) ions.

In addition to that, the simple Curie-Weiss law is unable to reproduce properly the χT values of 1 between 25 and 50 K, temperatures close to the Curie temperature. One possibility to model the magnetic susceptibility close to the magnetic transition is to take explicitly into account the fact that there are two distinct sub-networks in the $[\mathrm{Mn^{II}Cr^{III}(ox)_3}]$ layers. Thus, generalizing the model of Weiss molecular field, Néel proposed[4] the following expression for the magnetic susceptibility.

$\dfrac{1}{\chi(\gamma_{HS} = 0)} = \dfrac{T - \theta}{C} - \dfrac{\gamma}{T - \theta'}$. The best fit of the magnetic susceptibility between 25 K and 175 K has been obtained keeping the same values for C and θ taking γ and θ' respectively equal to -0.265 $\mathrm{cm^{-3}\ K\ mol}$ and 8.16 K. Calculating the difference between the χT values obtained for **1** and the preceding expression results in a difference in χT lower than 0.04 $\mathrm{cm^3\ K\ mol^{-1}}$ between 25 K and 175 K. Finally, γ_{HS} is calculated using the relation: $\gamma_{\mathrm{HS}} = [\chi T - \chi T(\gamma_{\mathrm{HS}} = 0)]/[\ \chi T(\mathrm{Fe^{III}\text{-}HS}) - \chi T(\mathrm{Fe^{III}\text{-}LS})]$; where the values of 4.38 and 0.6 $\mathrm{cm^3\ K\ mol^{-1}}$ have been taken for $\chi T(\mathrm{Fe^{III}\text{-}HS})$ and $\chi T(\mathrm{Fe^{III}\text{-}LS})$ respectively. γ_{HS} is plotted as a function of temperature, before and after irradiation, in figure 4.

---

[1] A. Altomare, M. C. Burla, M. Camalli, G. L. Cascarano, C. Giacovazzo, A. Guagliardi, A. G. G. Moliterni, G. Polidori, R. Spagna, *J. Appl. Cryst.*, 1999, **32**, 115-119.

[2] SHELXL-97: G. M. Sheldrick, University of Göttingen, Germany, **1997**.

[3] L. J. Farrugia, *J. Appl. Cryst.,* 1997, **32**, 837.

[4] L. Néel *Ann. Phys,* 1948, **3**, 137.